NANO LETTERS

2009
Vol. 9, No. 12
4133-4137

Charge Transfer Chemical Doping of Few Layer Graphenes: Charge Distribution and Band Gap Formation

Naeyoung Jung,*,† Namdong Kim,‡ Steffen Jockusch,† Nicholas J. Turro,† Philip Kim,‡ and Louis Brus†

Department of Chemistry and Department of Physics, Columbia University, New York, New York 10027

Received July 22, 2009; Revised Manuscript Received September 28, 2009

ABSTRACT

The properties of few layer (one layer (1 L) to four layer (4 L)) graphenes doped by adsorption and intercalation of Br_2 and I_2 vapors are investigated. The Raman spectra of the graphene G vibrations are observed as a function of the number of layers. There is no evidence for chemical reaction disrupting the basal plane π electron conjugation. Adsorption of bromine on 1 L graphene creates a high doped hole density, well beyond that achieved by electrical gating with an ionic polymer electrolyte. In addition, the 2D Raman band is completely quenched. The 2 L bilayer spectra indicate that the doping by adsorbed I_2 and Br_2 is symmetrical on the top and bottom layers. Br_2 intercalates into 3 L and 4 L graphenes. The combination of both surface and interior doping with Br_2 in 3 L and 4 L creates a relatively constant doping level per layer. In contrast, the G spectra of 3 L and 4 L with surface adsorbed I_2 indicate that the hole doping density is larger on the surface layers than on the interior layers and that I_2 does not intercalate into 3 L and 4 L. This adsorption-induced potential difference between surface and interior layers implies that a band gap opens in the bilayer type bands of 3 L and 4 L.

Single atomic layer graphene is a nearly optically transparent semimetal membrane, whose extreme physical strength[1] and high electron mobility at room temperature result from extensive electron conjugation and delocalization. Charge transfer to and from adsorbed species can shift[2,3] the graphene Fermi level by a large fraction of an electronvolt. Such adsorption-induced chemical doping adjusts the Fermi level without introducing substitutional impurities, or basal plane reactions, that interrupt the conjugated network. Adsorption-induced chemical doping may well become an important aspect of future graphene technologies. In graphenes consisting of only a few layers, chemical doping can result from both surface adsorption and intercalation between layers. In this study we use Raman spectroscopy to investigate the interplay between surface adsorption and intercalation in few layer graphenes exposed to Br_2 and I_2 vapors at room temperature.

Molecular intercalation into bulk graphite typically creates stable stoichiometric "stage" compounds (termed graphite intercalation compounds GICs). Bromine creates a stage 2 bulk GIC in which graphene bilayers (2 L) are separated by intercalated Br_2 layers.[4−7] Such intercalated Br_2 layers are thought to be structurally commensurate with neighboring graphene.[4] Raman scattering is a powerful nondestructive and noncontact analytical tool for study of both GICs and few layer graphenes. The bromine GIC Raman spectrum shows that the graphite G band is energy upshifted by hole doping, from 1580 cm^{-1} in pure graphite to 1612 cm^{-1} in the GIC. An intercalated anionic bromine band is also observed near 240 cm^{-1}, downshifted from 323 cm^{-1} in free Br_2. In contrast to Br_2, I_2 does not form a bulk GIC, possibly because the longer I_2 bond length does not allow a intercalation structure.[8]

Br_2 and I_2 are more electronegative than graphite and should dope graphene positively when adsorbed. I_2 adsorbs on and dopes carbon nanotubes,[9−12] fullerenes,[13] pentacene,[14,15] and polyacetylene.[16,17] Charge transfer from the carbon substrate creates iodide anions that react with excess neutral I_2 to form adsorbed I_3^-, and I_5^-; these species are directly detected as resonantly enhanced Raman bands at 108 and 165 cm^{-1}. We observe very strong I_3^- and I_5^- Raman signals upon exposure of few layer graphenes to iodine. However, this present paper will focus on the distribution of doped positive charge in the graphene: the iodine Raman spectra will be reported elsewhere.

Single and few layer graphene samples were deposited by mechanical exfoliation in air onto p-type Si wafer chips with 300 nm thick SiO_2 using adhesive tape. Before halogen exposure, the graphene samples were characterized by Raman to determine the number of layers in each piece. Halogen gas exposure was performed inside a conventional two

* Corresponding author, nj2153@columbia.edu.
† Department of Chemistry.
‡ Department of Physics.

10.1021/nl902362q CCC: $40.75
Published on Web 10/14/2009

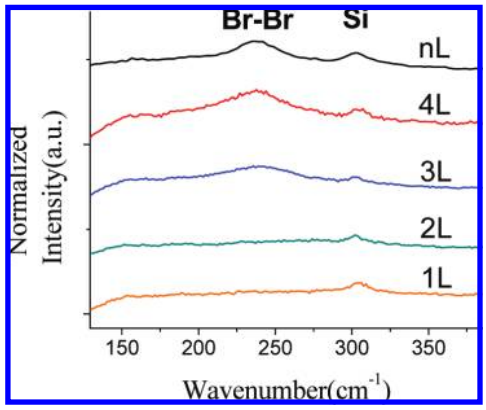

Figure 1. Br_2 stretching region Raman spectra for few layer graphenes exposed to bromine. The weak 303 cm^{-1} peak labeled Si is from the underlying crystalline silicon substrate. The Br−Br peak near 240 cm^{-1} is from intercalated bromine.

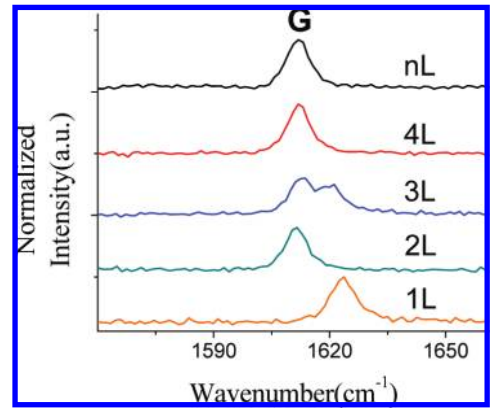

Figure 2. G peak Raman spectra of few layer graphenes exposed to bromine.

Table 1. G Peak Positions and fwhm Few Layer Graphenes Exposed to Br_2.[a]

	1 L	2 L	3 L	4 L	*n* L (bulk)
G peak position (cm^{-1}) ±0.5 cm^{-1}	1624	1612	1613[a], 1620[b]	1612	1612
Fermi energy (eV)	0.59	0.36	N/A	0.36	0.36
fwhm (cm^{-1})	6.6	5.7	6.0[a], 7.9[b]	5.6	5.5

[a] The 3 L spectra were fitted with Lorentzian lineshapes. Other spectra were fitted with Voigt functions. The instrumental broadening is 2.5 cm^{-1}. The Fermi energy calibration is extrapolated from Figure 3 of ref 25.

temperature zone glass sample tube initially evacuated to 2 × 10^{-5} Torr. A halogen reservoir was thermostated at 10 °C to establish a constant halogen vapor pressure in the cell. Liquid bromine was initially frozen and thawed several times to remove dissolved gases. All measurements were performed at room temperature. Typically graphene samples underwent a 1 h halogen exposure to reach equilibrium. Confocal backscattering Raman with a ca. 4 μm^2 spot size was observed, using a 40× objective focused through the cell window. 3.2mW of 633 nm He−Ne laser irradiation was used as the excitation source. The red 633 nm He−Ne laser was chosen to minimize Br_2 and I_2 electronic excitation, which is stronger at shorter wavelengths. The G mode peaks were fit with a Voigt function using a Gaussian instrumental function of 2.5 cm^{-1}

The graphene Raman D peak at 1350 cm^{-1} is an indicator of intrinsic defects, or basal plane chemical reaction that disrupts the π-conjugation and converts sp^2 C atoms to sp^3 C atoms. Our single and few layer graphene samples show essentially no D band upon exfoliation, indicating a high initial quality sample that is free of defects. This finding is typical of mechanically exfoliated samples. We also observe no D mode formation in one (1 L) to four layer (4 L) graphenes exposed to bromine or iodine vapors. This means that we detect no thermal or 633 nm laser-induced photochemical reaction under our experimental conditions. In previous basal plane oxidation and hydrogenation Raman studies, single layer (1 L) graphene was generally more reactive than few layer samples.[18,19]

Few layer graphenes are exposed to ca. 100 Torr Br_2 at room temperature. Figure 1 shows the resonantly enhanced, intercalated bromine stretching mode at 238 cm^{-1} in 3 L and 4 L graphene, and in the "bulk" many-layer (*n*L) sample. This is the same anionic bromine mode seen at 242 cm^{-1} in the stage 2 bulk GIC.[5] We do not detect the intercalated Br_2 stretching mode in 2 L graphene. No Raman bands due to physisorbed bromine species are detected; apparently because resonance enhancement for gas-phase-like, physisorbed Br_2 species should be weak at our laser wavelength 633 nm.

Charge transfer from physisorbed bromine species is evident in the graphene G mode spectra. The graphene G peak frequency is sensitive to charge doping which shifts the Fermi level away from the neutrality point.[20,21] The pristine graphene G peak at 1580 cm^{-1} is energy up-shifted with increasing doping.[22,23] This shift has been calibrated in electrical devices for 1 L and 2 L graphene.[20,21,24−26] In Figure 2, 1 L graphene exposed to Br_2 shows a very large energy upshift to 1624 cm^{-1}, significantly larger than the 1612 cm^{-1} G peak in the stage 2 bromine GIC.[27] This 44 cm^{-1} energy upshift from 1580 cm^{-1} is about 30% larger than the highest value achieved in top gating with ionic polymer electrolytes.[20] The calculated Fermi level shift is about 0.59 eV, this value is calculated as described in the caption of Table 1. The G mode full-width at half-maximum (fwhm) for 1 L is 6.6 cm^{-1}, which is almost 1 cm^{-1} larger than those of 2 L, 4 L, and bulk graphite. This 1 L G mode fwhm for doped samples is about the same as observed in back gate electrical devices, thus indicating that doping homogeneity is about the same in the two methods.

With 514 nm laser excitation, the strongest Raman transition in intrinsic suspended 1 L graphene is the 2D peak near 2800 cm^{-1}. Adsorption of 1 L graphene on SiO_2 decreases the 2D/G ratio by a factor of about 5.[28] Figure 3 shows essentially complete quenching of the 2D transition for Br_2-doped 1 L graphene on the oxide surface in our experiment at 633 nm laser excitation. The initial 2D/G integrated intensity ratio 1.32 on the substrate decreased to an upper limit of 0.001 upon exposure to Br_2. A qualitatively similar 2D/G decrease is reported for graphene multiple layers in solution with adsorbed doping species such as TCNE and TTF.[29,30] Theory predicts that the intensity of 2D

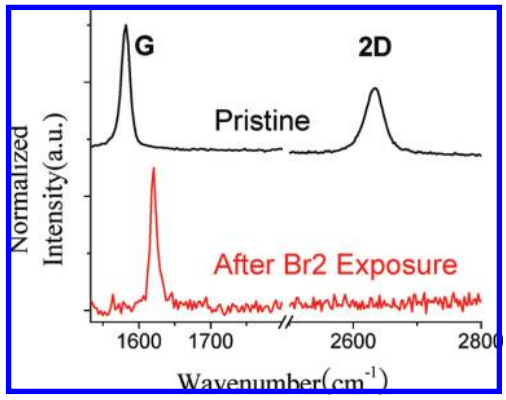

Figure 3. Low-resolution G and 2D Raman spectra for 1 L graphene before and after exposure to bromine.

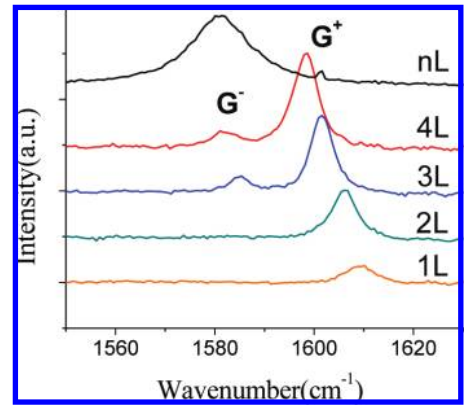

Figure 4. G peak Raman spectra of few layer graphenes and graphite, exposed to iodine vapor. Curves are vertically displaced. The relative intensity change from 1 L to graphite is shown. The G-peak fwhm of doped few layer graphene samples is smaller than that of the 1580 cm^{-1} undoped graphite G peak, as expected for doped samples. In graphite a small peak at 1601 cm^{-1} may represent the surface graphene layers with adsorbed I_2.

should decrease as electron−electron collisions increase strongly at high levels of doping.[31] The extreme environmental sensitivity shown by the 2D band in semimetallic graphene is quite remarkable and unique in molecular and materials Raman spectroscopy.

2 L, 4 L, and thicker bulklike graphenes show G spectra very similar to each other with a peak near 1612 cm^{-1}, lower than the 1 L G peak at 1624 cm^{-1}, but the same as the bulk GIC peak at 1612 cm^{-1}. The bilayer G mode Raman spectra have been theoretically analyzed by Ando and Koshino,[35] as a function of doping level, and layer inequivalence created by a perpendicular electric field. A perpendicular electric field breaks the inversion symmetry of the bilayer lattice and induces an energy gap.[32−37] As the gap opens, the Raman spectrum is predicted to show two G peaks (termed G^+ and G^-) with different shifts and intensities, corresponding to mixing of the (initially Raman active) symmetric and (initially Raman in-active) antisymmetric combination of G modes.[37] Our observation that 2 L exhibits only a single G band implies symmetric chemical doping. The two layers are physically equivalent. When the bilayer is deposited on a silicon dioxide substrate, asymmetric doping by adsorbed Br_2 is possible. Our observation supports symmetric doping and indicates that Br_2 diffuses efficiently along the interface between 2 L and the substrate. The greater G upshift and higher doping of 1 L compared to 2 L reflect hole doping from top and bottom adsorbed Br_2 layers on 1 L.

A simplified local Raman model has been historically used to understand the G spectra of bulk GICs.[7,38,39] Each graphene layer is assumed to produce one G peak whose upshift is simply determined by the two neighboring (either intercalant or graphene) layers. A graphene layer next to an intercalant layer has stronger doping and a larger upshift. Our 4 L structure has two bilayers separated by an intercalated bromine layer, with additional adsorbed bromine on top and bottom, as shown in Figure 5. The similarity in the 2 L and 4 L Raman spectra in Figure 2 suggest that the net doping effect from the intercalated Br_2 layer is very similar to that of the adsorbed Br_2 layers on top and bottom. Then, within the local model all graphene layers in 2 L, 4 L, and the bulk GIC would be equivalent, having neighboring graphene and Br_2 layers. Consistent with this model, 2 L, 4 L, and the bulk GIC do show a single G peak at 1612 cm^{-1}.

Table 2. G Peak Positions and fwhm of Few Layer Graphenes Exposed to I_2[a]

	1 L	2 L	3 L	4 L
G peak position (cm^{-1}) ±0.5 cm^{-1}	1608.8	1605.7	1584.9[a], 1601.6[b]	1581.8[a], 1598.3[b]
Fermi energy (eV)	0.43	0.32	N/A	N/A
fwhm (cm^{-1})	6.60	5.37	3.26[a], 4.72[b]	3.91[a], 5.28[b]

[a] 3 L and 4 L spectra were fitted with two different Lorentzian modes. The calibration of the Fermi energy level is taken from Figure 3 of ref 25.

Intercalated 3 L is the only intrinsically asymmetric structure for Br_2-doped graphene, since it does not possess reflection symmetry. Even if we consider adsorbed and intercalated Br_2 layers to be identical, 3 L has two types of physically inequivalent graphene layers. 3 L is also the only structure to show two G bands, at 1620 and 1613 cm^{-1}. Within the local interpretation, the higher energy peak at 1620 cm^{-1} is assigned to the shift for two Br_2 outside layers; this peak occurs at 1623 cm^{-1} in 1 L with adsorbed Br_2. The lower energy peak at 1612 cm^{-1} is assigned to the 2 L structural component of 3 L.

The G peak upshift of I_2-exposed graphene is less than that of Br_2-exposed graphene due to two reasons. A comparison of the molecular redox potentials indicates that iodine is a weaker oxidizing agent than bromine. Also at a given temperature iodine has a lower vapor pressure than bromine. Figure 4 and Table 2 show weaker chemical doping with a smaller G peak upshift for few layer graphenes exposed to about 0.1 Torr of I_2 vapor from the 10 °C iodine reservoir. With I_2 the Fermi level shift for 1 L is 0.43 eV, and the 2D band is essentially completely quenched as was the case for Br_2. The observation of only one G peak for 2 L implies that doping by adsorbed I_2 is symmetric on the bilayer top and bottom, similar to bromine-exposed 2 L. Our thick graphene sample shows a G peak at 1580 cm^{-1}, which is the value for bulk graphite without intercalation. Thus, as illustrated in Figure 5, we do not observe I_2 intercalation under our conditions; recall that I_2 does not form a bulk GIC either. The systematic downshift of the stronger G peak

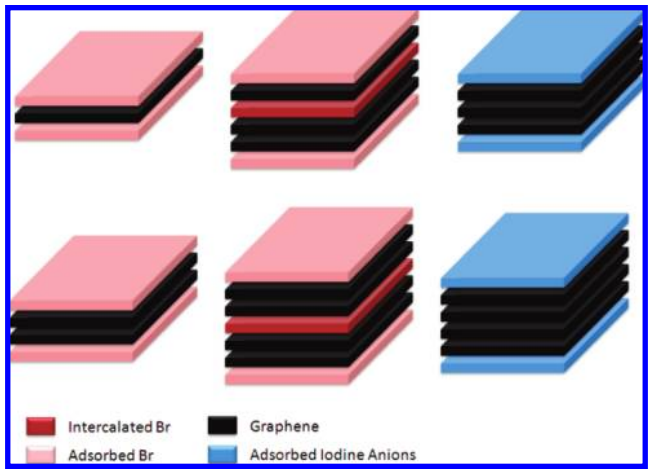

Figure 5. Schematic diagram of few layer graphenes exposed to Br_2 (left) and I_2 (right). On the left side the 3 L and 4 L structures have both intercalated (dark pink) and adsorbed (light pink) Br_2 layers. On the right side the 3 L and 4 L structures have surface adsorbed (light blue) iodine anion layers without intercalation.

frequency with increasing thickness also indicates that only the surface doping happens and intercalation does not occur.

From a comparison of Figures 2 and 4, the G spectra of 3 L and 4 L are seen to be very different for I_2 and Br_2. Both halogens dope the graphenes by surface adsorption. Only the Br_2 system has an additional doping Br_2 layer near the center, as shown schematically in Figure 5. For the I_2 system, within the local model there would be two discrete G peak shifts in 3 L and 4 L: one for inner layers adjacent to other graphene neighboring layers, and one for outer layers adjacent to adsorbed I_2 and one graphene neighboring layers. Their relative intensities should be given by the relative number of each type layer. In 3 L and 4 L this local model behavior is not observed for I_2. Rather, the higher peak marked G^+ is much stronger than the lower G^- peak. The G^+ peak position moves systematically in the 1 L to 4 L series. These spectra are similar to the predicted and observed 2 L Raman spectra involving unequally doped layers in the presence of a perpendicular electric field.[37,38] We propose that I_2 surface chemical doping in 3 L and 4 L creates higher hole doping on the surface layers. Doping decays with a finite screening length into the interior, with static potential differences from layer to layer. Layered graphene screening calculations actually show oscillations in the doped charge decay.[40] In 3 L and 4 L our proposed perpendicular electrostatic displacement vectors D appear in Figure 6. We assign the G spectra to stronger symmetric G^+ and weaker antisymmetric G^- combinations of E_{2g} phonon modes in surface and interior layers.

The 3 L electronic structure is composed of 1 L and 2 L type bands.[41] In the trilayer tight binding Hamiltonian a symmetric potential difference between the two surface layers and the one interior layer plays the same role as the asymmetric potential difference in the bilayer Hamiltonian.[41] This symmetric potential difference would open a band gap in the bilayer type bands of 3 L. It is likely that such a band gap exists in 3 L and 4 L due to surface I_2 adsorption. In the Ando and Koshino[35] single gate 2 L Raman calculation (ref 35, Figure 5a), the G^-/G^+ intensity ratio grows as the band gap opens. From the measured ca. 3/1 ratio in Figure 4, we can estimate a gap on the order of 0.1 eV in the 2 L type bands from their numerical modeling. This is only a rough estimate for our experiment; exact Raman modeling theory needs to be done for 3 L and 4 L type structures. Larger gaps could result from stronger doping. A recent photoemission study of surface chemical doping by potassium on bulk HOPG (highly ordered pyrolytic graphite) shows that a ~0.3 eV band gap opens near the surface.[42] Similarly we expect that a band gap in 3 L and 4 L could open for employing symmetric doping from top and bottom electrical gates in field effect devices.

In contrast, with Br_2 the combination of surface and interior doping creates a relatively constant doping density per layer, as evidenced by the presence of the same 1612 cm^{-1} line for 2 L and 4 L. This is the same doping level and upshift as in the bulk bromine GIC. Br_2 intercalates into 3 L graphene but not into 2 L. This same pattern is observed

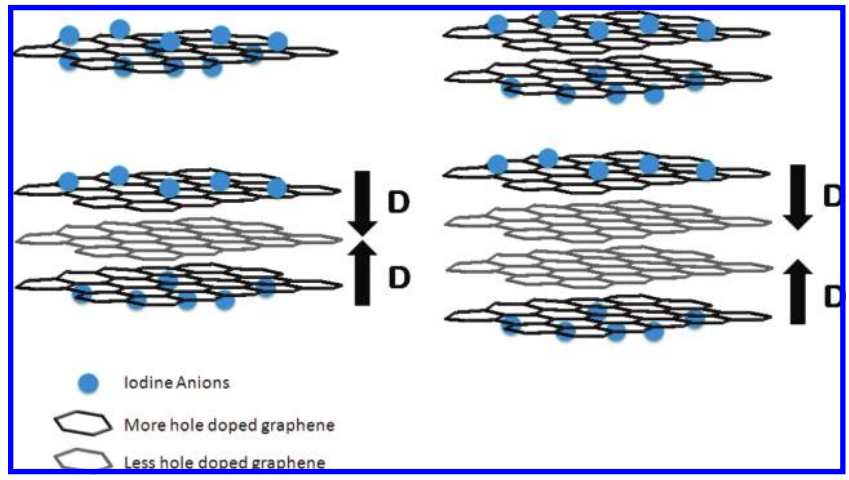

Figure 6. Schematic diagram of few layer graphenes doped by iodine adsorption. Surface iodine anions in blue dope holes preferentially into the surface graphene layers shown in black. Interior graphene layers in gray have less doping. The resulting perpendicular electric displacement vectors D are shown.

in the stage 2 bulk GIC. The energetics of this observation are intriguing and deserve further investigation.

In conclusion, our results show the potential for adsorption-induced charge transfer doping (including intercalation) to create adjustable doping patterns at high densities, in laterally large, few layer graphene samples without π-electron disruption. Surface doping creates a symmetric potential difference between surface and interior layers that can open a band gap in 2 L type bands. Further experimental and theoretical work is necessary on surface-doped and few layer graphenes to achieve a deeper understanding of the electronic and vibrational structure.

Acknowledgment. We thank Sunmin Ryu, Mark Hybertsen, Stephane Berciaud, Haitao Liu, Kwang Taeg Rim, and Michael Steigerwald for productive discussion of this research. This work was funded by the Department of Energy under Grant DE-FG02-98ER14861(L.E.B.) and by the National Science Foundation under No. DMR-0349232 (P.K.) and No. CHE-07-17518 (N.J.T.). We acknowledge financial support from the Nanoscale Science and Engineering Initiative of the National Science Foundation under NSF Award No. CHE-06-41523 and by the New York State Office of Science, Technology, and Academic Research (NYSTAR).

References

(1) Lee, C.; Wei, X. D.; Kysar, J. W.; Hone, J. *Science* **2008**, *321* (5887), 385–388.
(2) Wang, X. R.; Li, X. L.; Zhang, L.; Yoon, Y.; Weber, P. K.; Wang, H. L.; Guo, J.; Dai, H. J. *Science* **2009**, *324* (5928), 768–771.
(3) Schedin, F.; Geim, A. K.; Morozov, S. V.; Hill, E. W.; Blake, P.; Katsnelson, M. I.; Novoselov, K. S. *Nat. Mater.* **2007**, *6* (9), 652–655.
(4) Sasa, T.; Takahash, Y; Mukaibo, T. *Carbon* **1971**, *9* (4), 407-&.
(5) Eklund, P. C.; Kambe, N.; Dresselhaus, G.; Dresselhaus, M. S. *Phys. Rev. B* **1978**, *18* (12), 7069–7079.
(6) Erbil, A.; Dresselhaus, G.; Dresselhaus, M. S. *Phys. Rev. B* **1982**, *25* (8), 5451–5460.
(7) Song, J. J.; Chung, D. D. L.; Eklund, P. C.; Dresselhaus, M. S. *Solid State Commun.* **1976**, *20* (12), 1111–1115.
(8) Hooley, J. G. *Carbon* **1972**, *10* (2), 155-&.
(9) do Nascimento, G. M.; Hou, T.; Kim, Y. A.; Muramatsu, H.; Hayashi, T.; Endo, M.; Akuzawa, N.; Dresselhaus, M. S. *J. Phys. Chem. C* **2009**, *113* (10), 3934–3938.
(10) Zhou, W. Y.; Xie, S. S.; Sun, L. F.; Tang, D. S.; Li, Y. B.; Liu, Z. Q.; Ci, L. J.; Zou, X. P.; Wang, G.; Tan, P.; Dong, X.; Xu, B.; Zhao, B. *Appl. Phys. Lett.* **2002**, *80* (14), 2553–2555.
(11) Cambedouzou, J.; Sauvajol, J. L.; Rahmani, A.; Flahaut, E.; Peigney, A.; Laurent, C. *Phys. Rev. B* **2004**, *69* (23), 235422.
(12) Grigorian, L.; Williams, K. A.; Fang, S.; Sumanasekera, G. U.; Loper, A. L.; Dickey, E. C.; Pennycook, S. J.; Eklund, P. C. *Phys. Rev. Lett.* **1998**, *80* (25), 5560–5563.
(13) Limonov, M. F.; Kitaev, Y. E.; Chugreev, A. V.; Smirnov, V. P.; Grushko, Y. S.; Kolesnik, S. G.; Kolesnik, S. N. *Phys. Rev. B* **1998**, *57* (13), 7586–7594 .
(14) Brinkmann, M.; Videva, V. S.; Bieber, A.; Andre, J. J.; Turek, P.; Zuppiroli, L.; Bugnon, P.; Schaer, M.; Nuesch, F.; Humphry-Baker, R. *J. Phys. Chem. A* **2004**, *108* (40), 8170–8179.
(15) Cazayous, M.; Sacuto, A.; Horowitz, G.; Lang, P.; Zimmers, A.; Lobo, R. *Phys. Rev. B* **2004**, *70* (8), 081309.
(16) Wang, D. K.; Tsukamoto, J.; Takahashi, A.; Muraki, N.; Katagiri, G. *Synth. Met.* **1994**, *65* (2−3), 117–122.
(17) Marikhin, V. A.; Novak, I. I.; Kulik, V. B.; Myasnikova, L. P.; Radovanova, E. I.; Belov, G. P. *Phys. Solid State* **2002**, *44* (6), 1188–1195.
(18) Liu, L.; Ryu, S. M.; Tomasik, M. R.; Stolyarova, E.; Jung, N.; Hybertsen, M. S.; Steigerwald, M. L.; Brus, L. E.; Flynn, G. W. *Nano Lett.* **2008**, *8* (7), 1965–1970.
(19) Ryu, S.; Han, M. Y.; Maultzsch, J.; Heinz, T. F.; Kim, P.; Steigerwald, M. L.; Brus, L. E. *Nano Lett.* **2008**, *8* (12), 4597–4602.
(20) Das, A.; Pisana, S.; Chakraborty, B.; Piscanec, S.; Saha, S. K.; Waghmare, U. V.; Novoselov, K. S.; Krishnamurthy, H. R.; Geim, A. K.; Ferrari, A. C.; Sood, A. K. *Nat. Nanotechnol.* **2008**, *3* (4), 210–215.
(21) Yan, J.; Henriksen, E. A.; Kim, P.; Pinczuk, A. *Phys. Rev. Lett.* **2008**, *101* (13), 136805.
(22) Pisana, S.; Lazzeri, M.; Casiraghi, C.; Novoselov, K. S.; Geim, A. K.; Ferrari, A. C.; Mauri, F. *Nat. Mater.* **2007**, *6* (3), 198–201.
(23) Lazzeri, M.; Mauri, F. *Phys. Rev. Lett.* **2006**, *97* (26), 266406.
(24) Yan, J.; Zhang, Y. B.; Kim, P.; Pinczuk, A. *Phys. Rev. Lett.* **2007**, *98* (16), 166802.
(25) Das, A.; Chakraborty, B.; Piscanec, S.; Pisana, S.; Sood, A. K.; Ferrari, A. C. *Phys. Res. B* **2009**, *79* (15), 155417.
(26) Yan, J.; Zhang, Y. B.; Goler, S.; Kim, P.; Pinczuk, A. *Solid State Commun.* **2007**, *143* (1−2), 39–43.
(27) Dresselhaus, M. S.; Dresselhaus, G. *Adv. Phys.* **2002**, *51* (1), 1–186.
(28) Berciaud, S.; Ryu, S.; Brus, L. E.; Heinz, T. F. *Nano Lett.* **2009**, *9* (1), 346–352.
(29) Das, B.; Voggu, R.; Rout, C. S.; Rao, C. N. R. *Chem. Commun.* **2008**, (41), 5155–5157.
(30) Voggu, R.; Das, B.; Rout, C. S.; Rao, C. N. R. *J. Phys.: Condens. Matter* **2008**, *20* (47), 472204.
(31) Basko, D. M. *Phys. Rev. B* 2009, *79*, (12).
(32) McCann, E. *Phys. Rev. B* **2006**, *74* (16), 161403.
(33) Castro, E. V.; Novoselov, K. S.; Morozov, S. V.; Peres, N. M. R.; Dos Santos, J.; Nilsson, J.; Guinea, F.; Geim, A. K.; Neto, A. H. C. *Phys. Rev. Lett.* **2007**, *99*.
(34) Ohta, T.; Bostwick, A.; Seyller, T.; Horn, K.; Rotenberg, E. *Science* **2006**, *313* (5789), 951–954.
(35) Ando, T.; Koshino, M. *J. Phys. Soc. Jpn.* **2009**, *78* (3), 034709.
(36) Oostinga, J. B.; Heersche, H. B.; Liu, X. L.; Morpurgo, A. F.; Vandersypen, L. M. K. *Nat. Mater.* **2008**, *7* (2), 151–157.
(37) Malard, L. M.; Elias, D. C.; Alves, E. S.; Pimenta, M. A. *Phys. Rev. Lett.* **2008**, *101* (25), 257401.
(38) Underhill, C.; Leung, S. Y.; Dresselhaus, G.; Dresselhaus, M. S. *Solid State Commun.* **1979**, *29* (11), 769–774.
(39) Dresselhaus, M. S.; Dresselhaus, G.; Eklund, P. C.; Chung, D. D. L. *Mater. Sci. Eng.* **1977**, *31*, 141–152.
(40) Guinea, F. *Phys. Rev. B* **2007**, *75* (23), 235433.
(41) Koshino, M.; McCann, E. *Phys. Rev. B* **2009**, *79* (12), 125443.
(42) Kamakura, N.; Kubota, M.; Ono, K. *Surf. Sci.* **2008**, *602* (1), 95–101.

NL902362Q